JCTC Journal of Chemical Theory and Computation

Benchmarking the Conductor-like Polarizable Continuum Model (CPCM) for Aqueous Solvation Free Energies of Neutral and Ionic Organic Molecules

Yu Takano and K. N. Houk*

Department of Chemistry and Biochemistry, University of California, Los Angeles, 607 Charles E. Young Drive East, Los Angeles, California 90095-1569

Received June 17, 2004

Abstract: The conductor-like polarizable continuum model (CPCM) using several cavity models is applied to compute aqueous solvation free energies for a number of organic molecules (30 neutral molecules, 21 anions, and 19 cations). The calculated solvation free energies are compared to the available experimental data from the viewpoint of cavity models, computational methods, calculation time, and aqueous pK_a values. The HF/6-31+G(d)//HF/6-31+G(d) and the HF/6-31+G(d)//B3LYP/6-31+G(d) with the UAKS cavities, in which radii are optimized with PBE0/6-31G(d), provide aqueous solvation effects in best agreement with available experimental data. The mean absolute deviations from experiment are 2.6 kcal/mol. The MP2/6-31++G-(d,p)//HF/6-31+G(d) with the CPCM-UAKS(HF/6-31+G(d)) calculation is also performed for the base-catalyzed hydrolysis of methyl acetate in water.

Introduction

Many chemical and biological reactions occur in water, where the polar and ionic processes are much more favorable than in the gas phase. Many efforts have been devoted to the development of methods to compute reaction barriers and energetics occurring in condensed phases with experimental accuracy.[1] Effective explicit water models become available for the description of chemical systems in liquid solution.[1] However, with high-level quantum mechanics, only a limited number of solvent molecules can be included explicitly due to the high cost of the calculations.

The goal of this work is to determine which theoretical procedure provides the most quantitative estimate of aqueous solvation effects, so that the rates of chemical and biological reactions in water can be computed accurately. One of the most successful solvation models is the conductor-like polarizable continuum model (CPCM).[2] Here we benchmark different variations of CPCM for the computation of solvation energies of neutral and ionic organic species and compare them to several other works. The CPCM method has also been applied to the computation of the alkaline hydrolysis of methyl acetate in aqueous solution.

* Corresponding author e-mail: houk@chem.ucla.edu.

Background

Dielectric continuum theories[1] are now widely used to describe hydration in conjunction with quantum mechanical calculations due to the relatively low cost of the calculation. CPCM[2] and PCM[3] are two of many successful solvation models. In their approaches, the solute interacts with the solvent represented by a dielectric continuum model. The solute molecule is embedded into a cavity surrounded by a dielectric continuum of permittivity ϵ. The accuracy of continuum solvation models depends on several factors; the most important one is the use of proper boundary conditions on the surface of the cavity containing the solute. CPCM and PCM define the cavities as envelopes of spheres centered on atoms or atomic groups: a number of cavity models have been suggested. Inside the cavity the dielectric constant is the same as in vacuo, outside it takes the value of the desired solvent. Once the cavity has been defined, the surface is smoothly mapped by small regions, called tesserae. Each tessera is characterized by the position of its center, its area, and the electrostatic vector normal to the surface passing through its center. Recently, the CPCM method has been improved and extended in GAUSSIAN03[4a] so that the cavity can be selected in a number of different ways.

10.1021/ct049977a CCC: $30.25
Published on Web 11/13/2004

In CPCM, the solvation free energy can be expressed[1a]

$$\Delta G_{solv} = \Delta G_{el} + \Delta G_{cav} + \Delta G_{dis} + \Delta G_{rep} + RT \ln\left(\frac{q_{rot,g} q_{vib,g}}{q_{rot,s} q_{vib,s}}\right) - RT \ln\left(\frac{n_{solute,g} \Lambda_{solute,g}}{n_{solute,s} \Lambda_{solute,s}}\right) + P\Delta V \quad (1)$$

ΔG_{el} is the electrostatic component of ΔG_{solv}. The G_{el} term is calculated using the CPCM self-consistent reaction field (SCRF) method.[2] The cavitation term, ΔG_{cav}, is calculated with the expression derived by Pierotti from the hard sphere theory[5] and adapted to the case of nonspherical cavities.[3b] The dispersion and repulsion terms, ΔG_{dis} and ΔG_{rep}, are computed following Floris and Tomasi's procedure,[6] with the parameters proposed by Callet and Claverie.[7] The $q_{rot,g}$, $q_{vib,g}$, $q_{rot,s}$, and $q_{vib,s}$ are denoted the microscopic partition functions for rotational and vibrational states of the solute in the gas phase and in solution, respectively; $n_{solute,g}$ and $n_{solute,s}$ are the numeral densities of solute; and $\Lambda_{solute,g}$ and $\Lambda_{solute,s}$ are the momentum partition functions. The last term, $P\Delta V$, may be neglected since its value is normally less than 10^{-3} kcal/mol.[8] The quantity, $-RT \ln(n_{solute}\Lambda_{solute})$, is a free energy correction to account for solute occupying the entire volume available in the reference state. For simple models such as isotropic solutions with no chemical association or dissociation processes, this contribution is equal to zero. The term involving the vibrational and rotational degrees of freedom, $\ln(q_{vib,g}/q_{vib,s})$ and $\ln(q_{rot,g}/q_{rot,s})$, is negligible.[1a]

The last three terms in eq 1 are neglected in the PCM and CPCM formulations.[1a] It, however, has been noted that things are actually more complex when one considers dimers or trimers held together by relatively weak interactions and for chemical association or dissociation processes.[1a]

Computational Method

The CPCM-SCRF calculations[2] at the HF/6-31+G(d) and B3LYP/6-31+G(d) levels were carried out on the stationary points to address solvation effects. A dielectric constant of 78.39 was utilized in order to simulate aqueous environment. The CPCM calculations were performed with tesserae of 0.2 Å^2 average size. All structures were optimized at the HF/6-31+G(d) and B3LYP/6-31+G(d) levels[9−11] in the gas phase and at the B3LYP/6-31+G(d) level in the aqueous environment. All stationary points were characterized by frequency calculations at the same level. All calculations were carried out with GAUSSIAN03[4a] and GAUSSIAN98.[4b] We used 1 mol L^{-1} as the standard state for both the gas phase and the solution for all thermodynamic properties.

In CPCM and PCM, the choice of cavities is important because the computed energies and properties depend on the cavity size. In this study, the UA0, UAHF, UAKS, UFF, PAULING, and BONDI cavities were used to evaluate the aqueous solvation effects using CPCM and PCM. The UA0 cavity is built up using the united atom topological model (UATM)[8a] applied on atomic radii of the universal force field (UFF).[9] By default, the UA0 model is chosen to build the cavity in GAUSSIAN03.[14] The UAHF and UAKS cavities use UATM with radii optimized for the HF/6-31G(d) and PBE0/6-31G(d)[10] levels of theory, respectively. The UAHF model is the default cavity of GAUSSIAN98. A set of the radii from UFF is used for making the UFF cavities. For the PAULING and BONDI cavities, each solute atom and group is assigned van der Waals values obtained from Pauling[12b] or Bondi[12c] atomic radii.

Table 1. Mean Absolute Deviations (MADs) of the Aqueous Solvation Free Energies of 70 Neutral and Charged Molecules at the HF/6-31+G(d)//B3LYP/6-31+G(d) Level Using CPCM with Several Cavities[a]

	total	neutral	anion	cation
UAKS	2.61	1.35	3.21	3.93
UAHF(G03)	2.84	1.10	3.92	4.93
UAHF(G98)	2.95	1.43	3.86	4.32
BONDI	3.64	2.93	3.38	5.04
PAULING	3.67	3.49	2.73	4.98
UA0	7.62	2.75	9.64	13.09
UFF	8.10	2.82	9.30	15.12

[a] MADs are shown in kcal/mol.

Test of the Reliability of CPCM

Aqueous solvation free energies for a number of organic molecules (30 neutrals, 21 anions, and 19 cations) computed using the CPCM method.[2] We investigated the calculated solvation free energies compared to the available experimental data[16] from the viewpoint of cavities, computational methods, calculation time, and aqueous pK_a values. The computed aqueous solvation effects were also compared with solvation energies computed using COSMO,[2] cluster-continuum model,[17] SM5.42R,[18] PCM,[3] and IPCM methods.[19]

Cavity Models. Table 1 summarizes the mean absolute deviations (MADs) of the aqueous solvation free energies calculated with seven cavities at the HF/6-31+G(d)//B3LYP/6-31+G(d) level[9−11] from the experimental data[16] for 70 neutral and charged molecules.

CPCM with the new cavities, UAKS and UAHF(G03), has improved accuracy in the aqueous solvation energies for a set of 70 organic species, though these methods still do not achieve the accuracy of experimental data (0.2 kcal/mol for neutral molecules[20,21] and 2 kcal/mol for ions[16]). The MADs calculated by the CPCM-UAKS and CPCM-UAHF(G03) are 2.61 kcal/mol (1.35, 3.21, and 3.93 kcal/mol for 30 neutrals, 21 anions, and 19 cations, respectively) and 2.84 kcal/mol (1.10, 3.92, and 4.93 kcal/mol), respectively. On the other hand, the CPCM-UA0 and CPCM-UFF methods fail for charged molecules with MADs of 9.64 (13.09) and 9.30 (15.12) kcal/mol for anion (cation) solutes, respectively. The PAULING cavities show the best solvation free energies (2.73 kcal/mol) for anion molecules but give the worst agreement with experiment for neutrals. For all cavities but the PAULING cavities, the calculated solvation free energies for the neutral molecules are much closer to the experimental results than those for the charged species. The large solvation energy errors for the ions is due to inadequate treatment of specific short-range interactions, probably associated with strong hydrogen bonds between the ions and first-shell water molecules. Dielectric continuum theory[1] cannot account for short-range solute−solvent interactions such as hydrogen bond. In addition, since anions and cations have aqueous solvation free energies in the range of 60−110 kcal/mol in

Table 2. Mean Absolute Deviations (MADs) of the Aqueous Solvation Free Energies of 70 Neutral and Charged Molecules at the HF/6-31+G(d)//B3LYP/6-31+G(d), B3LYP/6-31+G(d)//B3LYP/6-31+G(d), and HF/6-31+G(d)//HF/6-31+G(d) Levels Using CPCM with the UAKS Cavities[a]

	HF//HF	HF//B3LYP	B3LYP//B3LYP
total	2.56	2.61	3.32
neutral	1.14	1.35	0.88
anion	3.10	3.21	5.64
cation	4.34	3.93	4.32

[a] MADs are shown in kcal/mol.

Table 3. Mean Absolute Deviations (MADs) of the Aqueous Solvation Free Energies of 70 Neutral and Charged Molecules at the HF/6-31+G(d)//B3LYP/6-31+G(d) Level Using CPCM with the UAKS Cavities[a,b]

	water	vacuo
total	2.60	2.61
neutral	1.79	1.35
anion	3.00	3.21
cation	3.60	3.93

[a] MADs are shown in kcal/mol. [b] The geometries were optimized in the water environment and in vacuo.

contrast to neutral molecules (0−10 kcal/mol), it is hard to achieve the 1 kcal/mol level of accuracy in prediction of the solvation free energy of ions.

Computational Methods. Table 2 shows the computational method dependence of MADs of the solvation free energy for the neutral and charged solutes. The geometries were optimized in the gas phase, and the UAKS cavities were used. The MADs of the solvation free energies at the HF/6-31+G(d)//B3LYP/6-31+G(d) level become 0.7 kcal/mol smaller than those at the B3LYP/6-31+G(d)//B3LYP/6-31+G(d) level. Especially, MADs of the solvation energies for the anion solutes are improved by 2.43 kcal/mol. There is a tendency that the cavity that reduces MADs of charged species increases the MADs of the neutral species. Optimization at the HF level provides MADs similar to those at the B3LYP level, indicating that optimized geometries using HF and B3LYP are close to each other.

Calculated MADs of the neutral and charged solutes with the geometries optimized in water are shown in Table 3. The geometries optimized in water make the MADs of charged species small while those for neutrals large. As a whole, optimization in water shows MADs similar to those in vacuo, implying that the optimized structures in water are similar to those in vacuo. In Table 4, the optimized geometrical parameters for some examples in vacuo and water are reported. It is apparent that the effect of reoptimization in water on the geometrical parameters are very small. However, some charged species failed to optimize geometries in water due to the dissociation of a proton, especially using the UAKS, UAHF, and PAULING cavities (Tables S10−S15).

The 6-31G, 6-31G(d), 6-31+G(d), 6-31+G(d,p), and 6-311+G(2d,p) basis sets were utilized to investigate the dependence on basis sets for aqueous solvation free energies. Even when basis sets are enlarged up to 6-311+G(2d,p), the MAD values from the experiment are very similar as shown in Table 5, indicating that diffuse and polarization functions of basis sets hardly change the aqueous solvation effects.

Calculation Time. Figure 1A shows the CPU time required to calculate the hydration energy using the previous (GAUSSIAN98)[4b] and the present (GAUSSIAN03)[4a] versions of the code. The present version provides a remarkable decrease of computational time because of the introduction of the fast multipole method to compute the solvation charge.

In Figure 1B, we compare CPCM to PCM with respect to the CPU time for the estimate of the aqueous solvation free energies in water. Although PCM is faster than CPCM for small molecules, CPCM is faster when the molecules become larger. In the CPCM approach, the electrostatic problem related to solute−solvent interaction can be solved with a

Table 4. Optimized Geometrical Parameters and Aqueous Solvation Free Energies for Some Sample Molecules in Vacuo and in Water

	CH_3O^-			CH_3OH			$CH_3NH_3^+$	
	vacuo	water		vacuo	water		vacuo	water
ΔG_{solv}[a]	−87.69	−88.53	ΔG_{solv}[a]	−6.23	−6.43	ΔG_{solv}[a]	−71.02	−72.59
R(C−O)[b]	1.34	1.40	R(C−O)[b]	1.43	1.43	R(C−N)[b]	1.52	1.50
R(O−H)[b]	1.14	1.11	R(C−H)[b]	1.10	1.10	R(C−H)[b]	1.09	1.09
∠COH[c]	115.6	113.0	R(O−H)[b]	0.97	0.98	R(N−H)[b]	1.03	1.04
			∠COH[c]	109.0	108.8	∠CNH[c]	111.6	111.6
			∠OCH[c]	112.0	111.6	∠NCH[c]	108.2	108.2

[a] ΔG_{solv}s are shown in kcal/mol. [b] Bond lengths are shown in Å. [c] Angles are shown in degrees.

Table 5. Mean Absolute Deviations (MADs) for the Aqueous Solvation Free Energies of 70 Neutral and Charged Molecules at the HF and B3LYP Levels Using CPCM-UAKS with Five Different Basis Sets[a]

		total	neutral	anion	cation			total	neutral	anion	cation
HF	6-31G	2.86	1.74	3.66	3.76	B3LYP	6-31G	2.95	0.91	4.63	4.31
	6-31G(d)	2.78	0.93	4.08	4.28		6-31G(d)	3.17	0.68	5.16	4.90
	6-31+G(d)	2.61	1.35	3.21	3.93		6-31+G(d)	3.32	0.88	5.64	4.32
	6-31+G(d,p)	2.56	1.38	3.19	3.72		6-31+G(d,p)	3.23	0.87	5.74	4.19
	6-311+G(2d,p)	2.77	1.49	3.52	3.95		6-311+G(2d,p)	3.28	0.75	5.92	4.37

[a] The geometries were optimized in vacuo at the B3LYP/6-31+G(d) level.

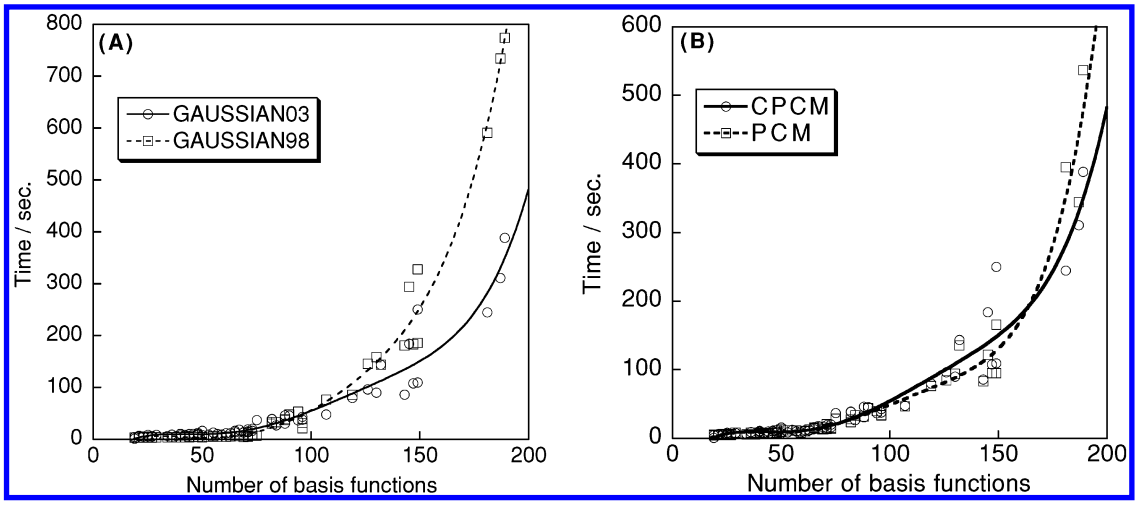

Figure 1. CPU times for the calculation of the aqueous solvation free energies at the HF/6-31+G(d) level by CPCM-UAKS using GAUSSIAN03 and GAUSSIAN98 (A) and by the CPCM-UAKS and PCM-UAKS methods using GAUSSIAN03 (B).

much simpler formalism than in PCM. This simpler formalism can be a faster estimate of the aqueous solvation free energies when larger systems are studied.

Aqueous pK_a. Aqueous pK_a values were evaluated using the B3LYP/6-31+G(d)//B3LYP/6-31+G(d) level of theory and inclusion of solvent effects at the HF/6-31+G(d) and B3LYP/6-31+G(d) levels. At present, many theoretical pK_a predictions have been reported.[17b,22] The vast majority of pK_a calculations use the direct definition shown in eq 2 with combination of the experimental data of the proton.[1c,22a−f]

$$HA \rightarrow H^+ + A^- \tag{2}$$

Since this reaction, however, involves the formation of charged species starting from neutral molecules, the procedure using eq 2 yields large errors due to imbalance of the charged and neutral species and requires the value of the experimental solvation free energy of the H^+ ion. By comparison, reactions that conserve the number of charged species are more suitable for accurate calculations of changes in solvation free energies. Pliego and Riveros used the proton-transfer reaction between the HA acids and hydroxide anion as shown in eq 3 along with the continuum-cluster method[17a] and compared their calculated values with the pK_a values calculated with the other solvation models. Since our objective is the benchmarking of the CPCM method, we made use of the reported results by Pliego and Riveros for comparison of the CPCM-UAKS and performed the pK_a calculations according to their procedure.[17b,22g,h]

$$HA + OH^- \rightarrow A^- + H_2O\ \Delta G^*_{sol} \tag{3}$$

The reaction (eq 3) conserves the number of charged species. The pK_a values were calculated according to eqs 4 and 5

$$pK_a(HA) = \frac{\Delta G^*_{sol}}{(2.303)RT} + 15.74 \tag{4}$$

$$\Delta G^*_{sol} = \Delta G^*_g + \Delta G^*_{solv}(A^-) + \Delta G^*_{solv}(H_2O) - \Delta G^*_{solv}(OH^-) - \Delta G^*_{solv}(HA) \tag{5}$$

where ΔG^*_g is the gas-phase reaction free energy (1 mol L^{-1} standard state) relative to eq 5, and $\Delta G^*_{solv}(X)$ is the solvation free energy of species X according to the Ben-Naim definition.[23]

The proton-transfer reaction as shown in eq 6 was used for the ionization of BH^+ acids

$$BH^+ + H_2O \rightarrow B + H_3O^+\ \Delta G^*_{sol} \tag{6}$$

The pK_a values for BH^+ acids can be expressed as

$$pK_a(BH^+) = \frac{\Delta G^*_{sol}}{(2.303)RT} - 1.74 \tag{7}$$

$$\Delta G^*_{sol} = \Delta G^*_g + \Delta G^*_{solv}(B) + \Delta G^*_{solv}(H_3O^+) - \Delta G^*_{solv}(H_2O) - \Delta G^*_{solv}(BH^+) \tag{8}$$

The calculated aqueous pK_a values for 27 species are listed in Table 6. CPCM provides MADs of the aqueous pK_a values of 2.83 and 2.47 pK_a units at the HF/6-31+G(d) and B3LYP/6-31+G(d) levels, respectively. The largest error occurs for $(CH_3COOC_2H_5)H^+$ and amounts to 6.32 and 6.55 pK_a units. The pK_a values estimated at the B3LYP/6-31+G(d) level are closer to experiment[16] than at the HF/6-31+G(d) level in contrast to the aqueous solvation free energy, indicating that accurate pK_a calculations require accurate gas-phase proton-transfer energies and solvation free energies.

Comparisons with Other Work. Our calculations have been also compared with other works as shown in Tables 7 and 8. We used the calculated data by Pliego and Riveros,[17] except for the CPCM[2] and COSMO[2] results. MADs of aqueous solvation free energies for 13 charged species are listed in Table 7. The higher accuracy of CPCM is observed and leads to a MAD of 3.04 kcal/mol, whereas the cluster-continuum,[17a] the COSMO,[2] the SM5.24R,[18] and the PCM methods[3] have MADs of about 10 kcal/mol. The IPCM method[19] shows the worst MAD of almost 20 kcal/mol. The failure of the cluster-continuum model can be traced to the continuum part of the calculation, specifically, the IPCM method. Improper cavities result in much larger MADs for the COSMO and PCM methods than for the CPCM method with appropriate cavity model, UAKS. PCM-UAKS provides

Table 6. Calculated and Experimental pK_a's in Water

compounds	pK_a(calc.) B3LYP[a]	pK_a(calc.) HF[b]	pK_a(exp.)	compounds	pK_a(calc.) B3LYP[a]	pK_a(calc.) HF[b]	pK_a(exp.)
CH_3CH_2O-**H**	21.80	20.93	15.90	H_2P-**H**	23.86	26.29	27
CH_3COO-**H**	5.47	6.62	4.76	C_6H_5O-**H**	12.63	13.10	9.99
CH_3O-**H**	21.12	21.54	15.50	C_6H_5S-**H**	7.31	8.18	6.62
H-Br	−12.10	−9.96	−8	CH_3CH_2OH-$\mathbf{H}^+$	−0.07	−0.38	−1.94
HCC-**H**	23.68	25.83	21.70	$(CH_3)_3N$-$\mathbf{H}^+$	11.69	11.36	9.80
HCOO-**H**	3.24	4.75	3.75	$(CH_3)_2C{=}O$-$\mathbf{H}^+$	−1.09	−1.61	−3.06
H-CN	10.28	12.51	9.22	$(CH_3COOC_2H_5)$-$\mathbf{H}^+$	−10.93	−11.16	−4.61
H-Cl	−10.79	−8.71	−6.10	$(CH_3)_2NH$-$\mathbf{H}^+$	11.89	11.58	10.73
H-F	0.68	1.40	3.18	CH_3NH_2-$\mathbf{H}^+$	10.37	10.09	10.66
H-OBr	11.37	14.93	8.60	CH_3OH-$\mathbf{H}^+$	−0.90	−1.45	−2.05
H-OCl	10.21	13.78	7.54	$(CH_3)_2O$-$\mathbf{H}^+$	−5.60	−6.13	−2.48
HO-**H**	15.74	15.84	15.74	H_3N-$\mathbf{H}^+$	9.17	8.99	9.25
HOO-**H**	16.35	19.20	11.65	$(C_6H_5COCH_3)$-$\mathbf{H}^+$	−8.32	−8.53	−3.87
HS-**H**	6.38	8.48	7.05	MAD	2.47	2.83	

[a] Electronic and aqueous solvation free energies are calculated at the B3LYP/6-31+G(d)//B3LYP/6-31+G(d) level. [b] Electronic energies are calculated at the B3LYP/6-31+G(d)//B3LYP/6-31+G(d) level, and aqueous solvation energies are estimated at the HF/6-31+G(d)//B3LYP/6-31+G(d) level.

Table 7. Comparison of the Aqueous Solvation Free Energy Calculated with CPCM,[a] Cluster-Continuum Model,[b] COSMO,[c] SM5.42R,[d] PCM,[e] and IPCM[f]

	CPCM	cluster−continuum	COSMO	SM5.42R	PCM	IPCM	Exp.
CH_3O^-	−87.69	−82.37	−81.22	−86.79	−79.98	−64.18	−95.2
Cl^-	−73.39	−67.94	−74.68	−77.05	−72.70	−61.80	−74.6
$HCOO^-$	−74.61	−63.77	−73.27	−75.22	−72.41	−60.81	−76.2
$C_2H_5O^-$	−84.93	−77.66	−77.61	−81.87	−76.70	−61.24	−91.1
OH^-	−106.57	−93.08	−96.29	−108.96	−92.14	−69.64	−105
$C_6H_5O^-$	−67.89	−68.60	*g*	−64.59	−63.78	−52.96	−71.3
SH^-	−70.37	−64.68	−72.12	−84.37	−71.04	−57.98	−71.6
CH_3S^-	−70.79	−63.87	−70.23	−78.97	−69.27	−56.58	−73.7
$CH_3CH_2OH_2^+$	−87.57	−75.71	−69.06	−74.04	−66.12	−66.48	−88.4
$CH_3NH_3^+$	−71.02	−72.69	−71.62	−76.03	−69.17	−68.83	−76.5
$CH_3OH_2^+$	−91.99	−84.64	−74.62	−79.82	−71.16	−72.24	−93.1
H_3O^+	−108.59	−101.87	−90.09	−92.51	−83.64	−88.77	−110.2
NH_4^+	−80.36	−79.38	−81.43	−87.03	−77.42	−77.56	−85.2
MAD	3.04	8.91	9.15	7.49	11.27	19.46	

[a] HF/6-31+G(d)//B3LYP/6-31+G(d) with UAKS cavities. [b] MP2/6-31+G(2df,2p)//HF/6-31+G(d,p). IPCM were used for the continuum part (ref 17a). [c] HF/6-31G(d)//B3LYP/6-31+G(d) with Klamt cavity model (SCRF=COSMORS). [d] HF/6-31G(d)//HF/6-31+G(d,p) (ref 17a). [e] HF/6-31G(d,p)//HF/6-31+G(d,p). The spheres defining the cavity were taken to be 1.2 times the van der Waals radii (ref 17a). [f] MP2/6-31+G(d,p)//HF/6-31+G(d,p). An isodensity of 0.0004 was used (ref 17a). [g] Not converged.

Table 8. Comparison of the Aqueous pK_a Values Calculated with CPCM,[a] Cluster-Continuum Model,[b] SM5.42R,[c] and PCM[d]

	CPCM	cluster−continuum	SM5.42R	PCM	exp.		CPCM	cluster−continuum	SM5.42R	PCM	exp.
CH_3CH_2O-**H**	21.80	16.08	25.93	16.52	15.90	C_6H_5O-**H**	12.63	7.19	16.98	4.50	9.99
CH_3COO-**H**	5.00	2.57	8.25	−3.27	4.76	CH_3CH_2OH-$\mathbf{H}^+$	−0.07	−4.16	0.17	1.74	−1.94
CH_3O-**H**	21.12	16.08	25.40	17.32	15.50	CH_3NH_2-$\mathbf{H}^+$	10.37	15.30	23.56	26.11	10.66
HCOO-**H**	2.83	1.03	4.30	−5.11	3.75	CH_3OH-$\mathbf{H}^+$	−0.90	−1.73	0.64	1.53	−2.05
H-Cl	−10.79	−9.25	−5.40	−13.47	−6.10	H_3N-$\mathbf{H}^+$	9.17	11.73	23.38	23.61	9.25
HS-**H**	6.38	5.69	2.33	0.35	7.05	MAD	2.19	2.06	6.20	6.91	

[a] B3LYP/6-31+G(d)//B3LYP/6-31+G(d) with UAKS cavities. [b] MP2/6-31+G(2df,2p)//HF/6-31+G(d,p). IPCM were used for the continuum part (ref 17b). [c] HF/6-31G(d)//HF/6-31+G(d,p) (ref 17b). [d] HF/6-31G(d,p)//HF/6-31+G(d,p). The spheres defining the cavity were taken to be 1.2 times the van der Waals radii (ref 17b).

MADs of 5.28 kcal/mol for 13 charged species. The IPCM method provides a very appealing approach to the problem of the cavity size. Unfortunately, besides the convergence problems that sometimes plague these methods, it seems that a single value for the density threshold is not adequate to reproduce experimental data, so that the problem of linking the atomic size to the molecular context remains.

Recently, Thompson, Cramer, and Truhlar presented a new continuum solvation model (SM5.43R) and compared it to the other solvation models including SM5.42R and CPCM.[20]

The MADs calculated by the SM5.43R, SM5.42, CPCM-UAHF(G03), and CPCM-UAHF(G98) were 0.51, 0.54, 1.07, and 1.08 kcal/mol for 257 neutrals and 4.65, 4.83, 4.57, and 5.90 kcal/mol for 47 ions, respectively. SM5.43R provides highly accurate aqueous solvation free energies for neutral species compared to experimental data. We cannot directly compare our calculated results to theirs, because they did not report what species were used for the calculation of the aqueous solvation energies, nor did they report the calculated aqueous solvation free energies. However, from Table 7, the MADs calculated by the CPCM-UAKS (3.04 kcal/mol) is a factor of 2.5 smaller than those calculated by the SM5.42R (7.49 kcal/mol) for 13 ions. Furthermore, they reported that the CPCM-UAHF(G98) gives smaller MADs than both the SM5.43R and SM5.42R for 47 ions. We found that a MAD calculated by CPCM-UAKS (3.5 kcal/mol) is smaller than that calculated by CPCM-UAHF(G98) (4.1 kcal/mol) for 40 ions (Table 1). These comparisons indicate that CPCM-UAKS is expected to give prediction of more accurate aqueous solvation energies for ions than SM5.42R and SM5.43R.

Table 8 lists the aqueous pK_a values for 11 species. The cluster-continuum model is the most reliable for the estimate of aqueous pK_a values and has a MAD of 2.06 pK_a units. Despite the lack of explicit water molecules, the CPCM method is also reasonable with an aqueous pK_a MAD of 2.19, but SM5.42R and PCM have much larger MADs (about 6 pK_a units). The worst computed aqueous pK_a values come from SM5.42R and PCM methods. Compared with the PCM method, the CPCM method provides much better calculated aqueous pK_a values because of the cavities used.

Application of the CPCM for Chemical Reactions

The base-catalyzed hydrolysis of methyl acetate in water[24,25] was investigated with the CPCM method. The hydrolysis of esters in basic solution stands out as one of the most studied reactions in chemistry because of its common occurrence in many organic and biochemical processes. In the base-catalyzed ester hydrolysis in water, with isolated methyl acetate and hydroxide ion (**Reactants**) as the starting materials, the approach of hydroxide ion to methyl acetate forms a tetrahedral intermediate (**Int**) through a transition state (**TS1**). Another barrier (**TS2**) is crossed to form the products, methanol and acetate ion (**Products**), via nonbarrier proton transfer.

Guthrie evaluated the free energy changes in this reaction using thermochemical and kinetic data.[24a] The calculated free energies for the five stationary points (**Reactants**, **TS1**, **Int**, **TS2**, and **Products**) have been compared to them.

The free energies for the base-catalyzed hydrolysis reaction of methyl acetate were calculated at the MP2/6-31++G(d,p)//HF/6-31+G(d) level. All the stationary points were obtained by full geometry optimizations in vacuo and characterized by harmonic frequency analysis. Zero point energies and thermal corrections at 298 K (scaled by 0.91)[26] were included in the reported energies. Solvation energies were computed using the CPCM-UAKS method at the HF/6-31+G(d) level using GAUSSIAN03.[4a] We used 1 mol L^{-1} as the standard state for both the gas phase and the solution for all thermodynamic properties.

Table 9. Calculated and Experimental Gibbs Free Energies for the Stationary Points of the Base-Catalyzed Hydrolysis of Methyl Acetate[a,b]

	ΔG(MP2)[c]	ΔG(exp.)
Reactants	0.0	0.0
TS1	21.3	18.5
Int	15.1	10.0
TS2	26.5	17.4
Products	−13.5	−14.4

[a] All Gibbs free energies relative to the isolated reactants. [b] All Gibbs free energies are shown in kcal/mol. Standard state of 1 mol L^{-1} for both gas phase and water phase thermodynamic properties. Correction factors ($-RT$ ln 2) were included for the enantiomeric minima and the transiton state structures. [c] MP2/6-31++G(d,p)//HF/6-31+G(d).

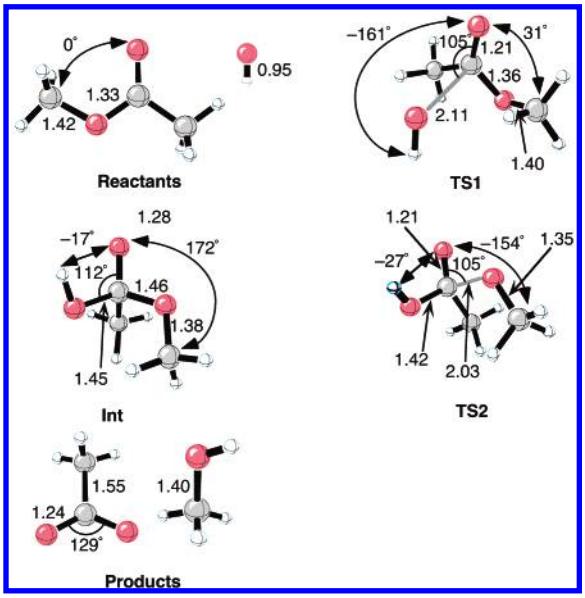

Figure 2. HF/6-31+G(d) geometries of **Reactants**, **TS1**, **Int**, **TS2**, and **Products** in the base-catalyzed hydrolysis of methyl acetate. Distances are in angstroms.

Table 9 shows the calculated and experimental free energies[24a] for the stationary points of the base-catalyzed hydrolysis of methyl acetate in water. The HF/6-31+G(d) geometries of the stationary points in the base-catalyzed hydrolysis of methyl acetate are illustrated in Figure 2. The calculated relative Gibbs free energy for **Products** reproduces the experimental value to 1 kcal/mol. In contrast, those for **TS1** and **Int** were overestimated by 2.8 and 5.1 kcal/mol. In the base-catalyzed hydrolysis of *N*,*N*-dimethylacetamide, Massova and Kollman estimated the free energy difference of 28.7 kcal/mol between the intermediate and the reactants using the PCM-UAHF(G98).[27] This values is about 10 kcal/mol larger than the experimental value of 19 kcal/mol.[28] Pliego and Riveros calculated an activation barrier (17.6 kcal/mol) close to experiment (18.6 kcal/mol),[24a] but this was because there was an equally high error in the calculations of the TS and reactants:[25e] the calculated solvation free energy of the hydroxide ion, −92.5 kcal/mol, gives an especially large deviation from experiment (−105.0 kcal/mol).[16a] CPCM-UAKS provides the reasonable solvation free energies

for the hydroxide ion (−105.5 kcal/mol). Compared to other methods, CPCM-UAKS gives an improved estimate of the activation barrier of hydrolysis but still overestimates it. An entropic correction in solution may be required for further improvement, because the CPCM total solute energy does not include an entropic change in solution as shown in eq 1. The ester hydrolysis involves association and dissociation processes, and the solute in this case is a transition state composed of two or more loosely bound molecules. The much larger deviation (about 10 kcal/mol) of **TS2** is likely due to the involvement of an explicit water molecule, which is proposed by previous theoretical works.[25] The accurate evaluation of the relative free energy for **TS2** must include an explicit water molecule.

Conclusions

Benchmarks of different variations of CPCM for the computation of solvation energies of neutral and ionic organic species have been performed and compared to other work in the literature. The CPCM-UAKS method provides the aqueous solvation free energies in agreement with experimental data and with improved computational times compared to other cavity methods. The mean absolute deviations from experiment are 2.6 kcal/mol. The largest solvation energy errors are obtained for anions and cations.

Acknowledgment. We are grateful to the National Science Foundation for financial support of this research. We also thank the National Computational Science Alliance under Grant MCA93S015N and the UCLA Advanced Technology Services for computational resources. We thank Fernando R. Clemente, Christophe Allemann, Andrew S. Dutton, Patrick R. McCarren, and Paul Ha Yeon Cheong for helpful discussions. Y.T. thanks the Japan Society for the Promotion of Science for a Research Fellowship for Young Scientists Abroad.

Supporting Information Available: Aqueous solvation free energies for 30 neutrals, 21 anions, and 19 cations (Tables S1−S27) and an example of an input file (Figure S1). This material is available free of charge via the Internet at http://pubs.acs.org.

References

(1) (a) Tomasi, J.; Persico, M. *Chem. Rev.* **1994**, *94*, 2027−2094. (b) Cramer, C. J.; Truhlar, D. G. *Chem. Rev.* **1999**, *99*, 2161−2200. (c) Chipman, D. M. *J. Phys. Chem. A* **2002**, *106*, 7413−7422. (d) Chipman, D. M. **2003**, *118*, 9937−9942.

(2) (a) Klamt, A.; Schüürmann, G. *J. Chem. Soc., Perkin Trans. 2* **1993**, 799. (b) Andzelm, J.; Kölmel, C.; Klamt, A. *J. Chem. Phys.* **1995**, *103*, 9312−9320. (c) Barone, V.; Cossi, M. *J. Phys. Chem. A* **1998**, *102*, 1995−2001. (d) Cossi, M.; Rega, N.; Scalmani, G.; Barone, V. *J. Comput. Chem.* **2003**, *24*, 669−681.

(3) (a) Miertus, S.; Scrocco, E.; Tomasi, J. *Chem. Phys.* **1981**, *55*, 117−129. (b) Barone, V.; Cammi, R.; Tomasi, J. *Chem. Phys. Lett.* **1996**, *255*, 327−335. (c) Cossi, M.; Scalmani, G.; Rega, N.; Barone, V. *J. Chem. Phys.* **2002**, *117*, 43−54. (d) Barone, V.; Improta, R.; Rega, N. *Theor. Chem. Acc*. **2004**, *111*, 237−245.

(4) (a) Frisch, M. J.; Trucks, G. W.; Schlegel, H. B.; Scuseria, G. E.; Robb, M. A.; Cheeseman, J. R.; Montgomery, J. A., Jr.; Vreven, T.; Kudin, K. N.; Burant, J. C.; Millam, J. M.; Lyengar, S. S.; Tomasi, J.; Barone, V.; Mennucci, B.; Cossi, M.; Scalmani, G.; Rega, N.; Petersson, G. A.; Nakatsuji, H.; Hada, M.; Ehara, M.; Toyota, K.; Fukuda, R.; Hasegawa, J.; Ishida, M.; Nakajima, T.; Honda, Y.; Kitao, O.; Nakai, H.; Klene, M.; Li, X.; Knox, J. E.; Hratchian, H. P.; Cross, J. B.; Adamo, C.; Jaramillo, J.; Gomperts, R.; Stratmann, R. E.; Yazyev, O.; Austin, A. J.; Camml, R.; Pomelli, C.; Ochterski, J. W.; Ayala, P. Y.; Morokuma, K.; Voth, G. A.; Salvador, P.; Dannenberg, J. J.; Zakrzewski, V. G.; Dapprich, S.; Daniels, A. D.; Strain, M. C.; Farkas, O.; Malick, D. K.: Rabuck, A. D.; Raghavachari, K.; Foresman, J. B.; Ortiz, J. V.; Cui, Q.; Baboul, A. G.; Clifford, S.; Cioslowski, J.; Stefanov, B. B.; Liu, G.; Liashenko, A.; Piskorz, P.; Komaromi, I.; Martin, R. L.; Fox, D. J.; Keith, T.; Al-Laham, M. A.; Peng, C. Y.; Nanayakkara, A.; Challacombe, M.; Gill, P. M. W.; Johnson, B.; Chen, W.; Wong, M. W.; Gonzalez, C.; Pople, J. A. Gaussian 03, revision B.04; Gaussian, Inc.: Pittsburgh, PA, 2003. (b) Frisch, M. J.; Trucks, G. W.; Schlegel, H. B.; Scuseria, G. E.; Robb, M. A.; Cheeseman, J. R.; Zakrzewski, V. G.; Montgomery, J. A., Jr.; Stratmann, R. E.; Burant, J. C.; Dapprich, S.; Millam, J. M.; Daniels, A. D.; Kudin, K. N.; Strain, M. C.; Farkas, O.; Tomasi, J.; Barone, V.; Cossi, M.; Cammi, R.; Mennucci, B.; Pomelli, C.; Adamo, C.; Clifford, S.; Ochterski, J.; Petersson, G. A.; Ayala, P. Y.; Cui, Q.; Morokuma, K.; Malick, D. K.; Rabuck, A. D.; Raghavachari, K.; Foresman, J. B.; Cioslowski, J.; Ortiz, J. V.; Baboul, A. G.; Stefanov, B. B.; Liu, G.; Liashenko, A.; Piskorz, P.; Komaromi, I.; Gomperts, R.; Martin, R. L.; Fox, D. J.; Keith, T.; Al-Laham, M. A.; Peng, C. Y.; Nanayakkara, A.; Challacombe, M.; Gill, P. M. W.; Johnson, B.; Chen, W.; Wong, M. W.; Andres, J. L.; Gonzalez, C.; Head-Gordon, M.; Replogle, E. S.; Pople, J. A. Gaussian 98, revision A.9; Gaussian, Inc.: Pittsburgh, PA, 1998.

(5) Pierotti, R. A. *Chem. Rev.* **1976**, *76*, 717−726.

(6) (a) Floris, F. M.; Tomasi, J. *J. Comput. Chem.* **1989**, *10*, 616−627. (b) Floris, F. M.; Tomasi, J.; Pascual-Ahuir, J. L. *J. Comput. Chem.* **1991**, *12*, 784−791.

(7) Caillet, J.; Claverie, P.; Pullman, B. *Acta Crystallgr.* **1978**, *B34*, 3266−3272.

(8) Ben-Naim, A.; Marcus, Y. *J. Chem. Phys.* **1984**, *81*, 2016−2027.

(9) (a) Becke, A. D. *Phys. Rev. A* **1988**, *38*, 3098−3100. (b) Lee, C.; Yang, W.; Parr, R. G. *Phys. Rev. B* **1988**, *37*, 785−789. (c) Becke, A. D. *J. Chem. Phys*. **1993**, *98*, 5648−5652.

(10) (a) Mclean, A. D.; Chandler, G. S. *J. Chem. Phys.* **1980**, *72*, 5639−5648. (b) Krishnan, R.; Binkley, J. S.; Seeger, R.; Pople, J. A. *J. Chem. Phys.* **1980**, *72*, 650−654.

(11) (a) Clark, T.; Chandrasekhar, J.; Spitznagel, G. W.; Schleyer, P. v. R. *J. Comput. Chem.* **1983**, *4*, 294−301. (b) Frisch, M. J.; Pople, J. A.; Binkley, J. S. *J. Chem. Phys.* **1984**, *80*, 3265−3269.

(12) (a) Barone, V.; Cossi, M.; Tomasi, J. *J. Chem. Phys.* **1997**, *107*, 3210−3221. (b) *Handbook of Chemistry and Physics*; Weast, R. C., Ed.; Chemical Rubber: Cleveland, OH, 1981. (c) Bondi, A. *J. Chem. Phys.* **1964**, *68*, 441−451.

(13) Rappé, A. K.; Casewit, C. J.; Colwell, K. S.; Goddard, W. A., III; Skiff, W. M. *J. Am. Chem. Soc.* **1992**, *114*, 10024−10035.

(14) GAUSSIAN03 online manual of the PCM and CPCM: http://www.gaussian.com/g_ur/k_scrf.htm

(15) Adamo, C.; Barone, V. *J. Chem. Phys.* **1999**, *110*, 6158−6170.

(16) (a) Pliego, J. R., Jr.; Riveros, J. M. *Phys. Chem. Chem. Phys.* **2002**, *4*, 1622−1627. (b) Williams, R. taken from: http://icg.harvard.edu/~chem206/Fall_2001/lectures/18_Acid_Based-_Properties_of_Organic_Molecules/pKa_compilation.pdf.

(17) Cluster-continuum is a hybrid approach that combines gas-phase clustering by explicit solvent molecules and solvation of the cluster by the dielectric continuum: (a) Pliego, J. R., Jr.; Riveros, J. M. *J. Phys. Chem. A* **2001**, *105*, 7241−7247. (b) Pliego, J. R., Jr.; Riveros, J. M. *J. Phys. Chem. A* **2002**, *106*, 7434−7439.

(18) (a) Li, J.; Hawkins, G. D.; Liotard, D. A.; Cramer, C. J.; Truhlar, D. G. *Chem. Phys. Lett.* **1998**, *288*, 293−298. (b) Giesen, D. J.; Hawkins, G. D.; Liotard, D. A.; Cramer, C. J.; Truhlar, D. G. *Theor. Chem. Acc.* **1997**, *98*, 85−109. (c) Chambers, C. C.; Cramer, C. J.; Truhlar, D. G. *J. Phys. Chem.* **1996**, *100*, 16385−16398. (d) Cramer, C. J.; Truhlar, D. G. *Science* **1992**, *256*, 213−217.

(19) Foresman, J. B.; Keith, T. A.; Wiberg, K. B.; Snoonian, J.; Frisch, M. J. *J. Phys. Chem.* **1996**, *100*, 16098−16104.

(20) Thompson, J. D.; Cramer, C. J.; Truhlar, D. G. *J. Phys. Chem. A* **2004**, *108*, 6532−6542. In this paper, the authors mentioned that they used the default setting of GAUSSIAN98 and GAUSSIAN03 and that the cavity was built by the UAHF method. They, however, performed the CPCM calculation with older version of GAUSSIAN03 (revision A.01). It should be noted that the later and latest versions of GAUSSIAN03 (revision B and revision C) build the cavity by the UA0 method. If the reader would like to use the cavity built by the UAHF method in the CPCM or PCM calculation, it is necessary to use the option, RADII=UAHF as shown in Supporting Information (Figure S1).

(21) (a) Rohschneider, L. *Anal. Chem.* **1973**, *45*, 1241−1247. (b) Park, J. H.; Hussam, A.; Couasnon, P.; Friz, D.; Carr, P. W. *Anal. Chem.* **1987**, *59*, 1970−1976.

(22) (a) Liptak, M. D.; Gross, K. C.; Seybold, P. G.; Feldgus, S.; Shields, G. C. *J. Am. Chem. Soc.* **2002**, *124*, 6421−6427. (b) Liptak, M. D.; Shields, G. C. *J. Am. Chem. Soc.* **2001**, *123*, 7314−7319. (c) Kallies, B.; Mitzner, R. *J. Phys. Chem. B* **1997**, *101*, 2959−2967. (d) Lopez, X.; Schaefer, M.; Dejaegere, A.; Karplus, M. *J. Am. Chem. Soc.* **2002**, *124*, 5010−5018. (e) Klici'c, J. J.; Friesner, R. A.; Liu, S.-Y.; Guida, W. C. *J. Phys. Chem. A* **2002**, *106*, 1327−1335. (f) Fu, Y.; Liu, L.; Li, R.-Q.; Liu, R.; Guo, Q.-X. *J. Am. Chem. Soc.* **2004**, *126*, 814−822. (g) Klamt, A.; Eckart, F.; Diedenhofen, M.; Beck, M. E. *J. Phys. Chem. A* **2003**, *107*, 9380−9386. (h) Almerindo, G. I.; Tondo, D. W.; Pliego, J. R., Jr. *J. Phys. Chem. A* **2004**, *108*, 166−171.

(23) Ben-Naim, A. *J. Phys. Chem.* **1978**, *82*, 792−803.

(24) (a) Guthrie, J. P. *J. Am. Chem. Soc.* **1973**, *95*, 6999−7003. (b) Bender, M. L. *Chem. Rev.* **1960**, *60*, 53−113. (c) Jencks, W. P. *Chem. Rev.* **1972**, *72*, 705−718. (d) *Ester Formation and Hydrolysis*; Bamford, C. H., Tipper, C. F. H., Eds.; Elsevier Science: Amsterdam, 1972; Vol. 10.

(25) (a) Hæffner, F.; Hu, C.-H.; Brinck, T.; Norin, T. *J. Mol. Struct. (THEOCHEM)* **1999**, *459*, 85−93. (b) Zhan, C.-G.; Landry, D. W.; Ornstein, R. L. *J. Am. Chem. Soc.* **2000**, *122*, 2621−2627. (c) Zhan, C.-G.; Landry, D. W.; Ornstein, R. L. *J. Phys. Chem. A* **2000**, *104*, 7672−7678. (d) Pliego, J. R., Jr.; Riveros, J. M. *Chem. Eur. J.* **2002**, *8*, 1945−1953. (e) Pliego, J. R., Jr.; Riveros, J. M. *J. Phys. Chem. A* **2004**, *108*, 2520−2526.

(26) (a) Bauschlicher, C. W.; Partridge, H. *J. Chem. Phys.* **1995**, *103*, 1788−1791. (b) Wong, M. W. *Chem. Phys. Lett.* **1996**, *256*, 391−399. (c) Scott, A. P.; Radom, L. *J. Phys. Chem.* **1996**, *100*, 16502−16513.

(27) Massova, I.; Kollman, P. A. *J. Phys. Chem. B* **1999**, *103*, 8628−8638.

(28) Guthrie, J. P. *J. Am. Chem. Soc.* **1974**, *96*, 3608−3615.

CT049977A